STATISTICAL CORRELATIONS IN THE PERMEABILITY TENSOR

Laura M. McGrath, Qiang Liu and Richard S. Parnas

Institute of Materials Science: Polymer Program, University of Connecticut, Storrs, CT, 06269, USA: rparnas@ims.uconn.edu

ABSTRACT: The determination of accurate permeability values is critical to process simulations for Resin Transfer Molding (RTM). New instrumentation was developed for high throughput permeability measurements. The design extends the work of Hoes [1] with new sensor design, much larger sensor pattern, and new analysis software. The new set-up was used to measure the permeability of a basalt woven 3/1 twill fabric. A comparison with previous work on 2/2 twill and plain woven fabrics reveals a relationship between the breadth of the anisotropy distribution, the principal components of the permeability tensor and fabric structure. This relationship has implications for manufacturing reliability, and may help explain why certain fabrics process much more consistently than others do.

KEYWORDS: Permeability, Reliability

INTRODUCTION

Accurate permeability values are extremely important for resin flow simulation and mold design in resin transfer molding (RTM). RTM has gained rapid acceptance [2] among composite processing techniques for its ability to mold large, complex shaped parts with a good surface finish. Yet, problems often occur due to non-uniform impregnation, void and dry spot formation [3], and lengthy impregnation cycles. If the permeability is known, the flow behavior can be properly computed as well as the mold clamping pressure, strength of the mold for shape retention [4] and pressure distributions in the mold.

Permeability is dependent on the pore geometry of the porous filler media of the composite [5]. Analytical models [6] have been developed to calculate the permeability of fabric materials yet they often do not take into account the actual complexity of the pore geometry. Numerical models are either very computationally intensive [7] or need time-consuming acquisition of the 3-D pore structure [8].

Permeability values are primarily obtained by experimentation via unidirectional flow (UD) methods (saturated or unsaturated) [9] or radial flow methods [9a, 9c, 9d]. In the UD flow experiments, permeability values in a specified direction are measured. In a saturated UD experiment, the fabric is compressed in a mold and the test fluid is forced through the mold. The flow rate and the pressure drop are recorded versus the length of the mold at steady-state [9a]. Whereas, in an unsaturated UD experiment, the fluid flows through the dry fiber bed, replacing the air present in the material. UD experiments are susceptible to edge effect errors (*i.e.* the fluid prefers the path of least resistance: flowing through the space devoid of fabric at the mold wall). Another drawback is that at least three measurements must be done to fully characterize the in-plane permeability tensor.

The radial test (or 2D test) can only be used with unsaturated flow methods. Fluid is injected into the center of the mold under either constant injection flow rate or constant injection pressure. The fluid superficial velocity can be determined with a transparent top plate and a video camera. The main advantage of the 2D test is that it allows the determination of both the in-plane permeability components and their angle in one single experiment [1].

The work presented here builds on the work of Hoes et al. [10], in which we have constructed a 2D unsaturated experimental set-up with two stiff metal plates and electrical sensors which record the flow front progression as a function of time. The apparatus presented supports a highly automated system that can be replicated with high frequency (5-10 per hr). As permeability is a statistically distributed parameter it can only be characterized by multiple experiments. With improved test frequency, we are now able to address the large standard deviation that prevails in permeability reporting. The rapid measurement methods also allow statistical corroborations to be made of the effects of fabric structure and anisotropy on permeability.

EXPERIMENTAL

Materials

The permeability measurements, replicated 64 times, were obtained for 6 layers of preformed basalt fabric, twill 3/1, from Albarrie Co., Canada. The properties are shown in Table 1. The 6 layers compressed to 4.661 mm in thickness resulting in a fiber vol. % of 35.8%. Data from the bottom and top plates are analyzed individually, in order to discern any non-uniformities in the vertical distribution of fluid. The angle, θ, between the warp direction of the fabric and the permeability principle axis is reported.

Three glass fabrics (Syncoglas R420, Syncoglas RE144/255, and CNF crowfoot) (Table 1) were also tested to verify the operation of our apparatus and to compare with previous work [1, 8, 9a].

Table 1. Properties of fabrics used in permeability measurements

Properties	Basalt Fabric	Syncoglas R420	Syncoglas RE144/255	CNF crowfoot
Areal Density, g/m^2	750	420	380	2900
Fiber Density, g/cm^3	2.7	2.52	2.52	2.52
Warp Yarn Linear Density, tex (g/km)	660	600	310	66.14
Weft Yarn Linear Density, tex (g/km)	330	600	580	33.07
Weave pattern	Twill 3/1	Plain weave 1/1	Twill 2/2	Twill 3/1
Yarn #/10 cm in warp	59.5	36.0	45	220
Yarn #/10 cm in weft	78	34.0	40.8	213

The permeability measurements were conducted with diluted corn syrup (DCS), (DI H$_2$O:'Nugget' brand light corn syrup, 11:3). The DCS has a viscosity near 0.1 Pa·s at room

temperature and is Newtonian in the shear rate ranges used in experimentation. The average viscosity of the DCS before and after experimentation was used.

Sensor Design

Electrical sensors made from a piece of copper wire with nylon insulation were fixed into the mold plate through a small screw. An O-ring is compressed when the sensor is screwed into the plate, sealing the mold and locking the sensor wire into place. The design permits the sensor to be slightly recessed below the plate level if desired which allows the permeability measurement of electrically conductive fabric. The sensor plate is placed at a low electrical potential (e.g. 5V). Thus, when an electrically non-conductive fabric is used in combination with a conductive test fluid, the fluid will generate a conductive bridge between the plate and the sensor core. This allows the flow front progression to be recorded as a function of time.

The back end of the copper wire is soldered to a ribbon cable leading to data acquisition cards in the computer. Two cards (National Instruments PCI-DIO 96), one for each plate, are used. There are 96 digital channels on each card, permitting 96 sensors in each plate. In the center of the top plate, a sensor is positioned to detect the incoming fluid and to begin the experiment clock.

Mold Design

Stainless steel mold plates, 40 cm long, 40 cm wide, and 3.2 cm thick (Figure 1) were designed with channels 1.9 cm wide (in the rear of each plate) at angle increments of 22.5°. Either 6 or 7 sensors are evenly spaced and inserted into the channels through the mold wall to detect fluid flow.
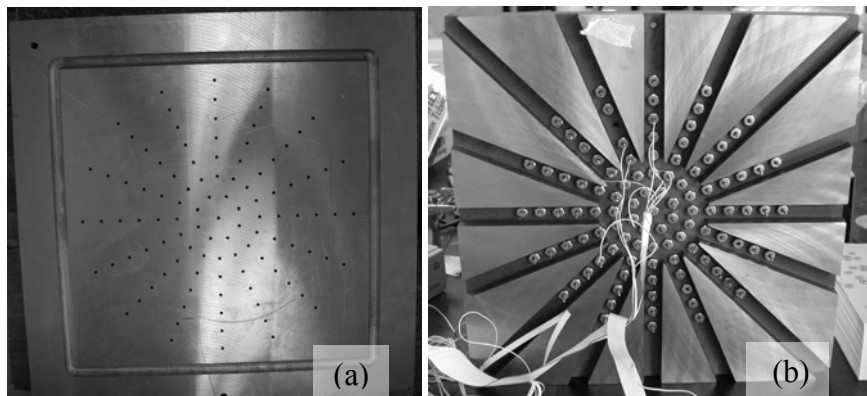

Figure 1. Top mold plate with mounted sensors (a) front view and (b) rear view

The bottom plate is the same as the top plate with the exception of a fluid injection port in the center. A hole of the same size as the injection port is punched in the middle of the fabric to allow uniform fluid penetration throughout the perform thickness.

Fluid Injection and Data Acquisition

The unsaturated 2D permeability experiment is conducted at a constant flow rate. The fluid is pumped into the mold by a Masterflex I/P pump (model no. 77601-10) through a flow meter and a control valve. A pressure transducer is positioned in the injection tube just below the surface of the sensor plate to measure the injection pressure and is connected to the PC. The experiment is monitored and controlled through Labview software which provides the permeability in a few seconds after the experiment concludes. The sensor trigger times from the top plate and from the bottom plate can be collected and analyzed separately to check for flow non-uniformity across the preform thickness.

Data Analysis

Data acquired from permeability experiments was derived in order to determine the flow pattern and the in-plane permeability tensor. The flow pattern, obtained from sensor trigger times, provides the shape of the advancing elliptical flow front, i.e., the angle of the permeability principle axes or the anisotropic ratio of the elliptical flow front. As the flow front is represented by an ellipse (Figure 2), the data acquired is used to determine the angle θ and the ratio a/b.
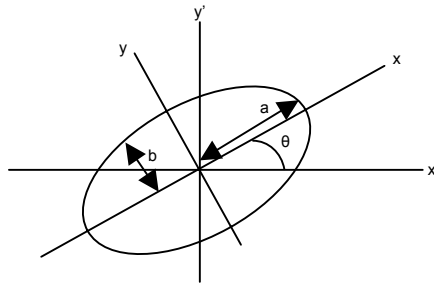

Figure 2. Ellipse representing the fluid flow front, with x' and y' as the lab coordinates

Labview data acquisition program establishes the sensor trigger time as the elapsed time from when the fluid hits the center sensor on the top plate (time = t_o) until the fluid triggers each sensor (time = t). When the flow front hits any sensor at time t, the distance between that sensor and the plate center, d, can be expressed as:

$$d = \sqrt{\frac{(m_1 t + r_o^2 + c)(1 + \tan^2(\alpha - \theta))}{\frac{1}{a/b} + \frac{a}{b}\tan^2(\alpha - \theta)}} \qquad (1)$$

Where:
α = angle between sensor line and lab coordinate axis x'
r_o = radius of injection hole, 3.188 mm
c = constant, accounts for uncertainty in the initial conditions at $t = 0$.
t = time at which a sensor is triggered

And m_1 is a function of flow rate and fabric properties:

$$m_1 = \frac{Q}{\pi h \phi} \tag{2}$$

Where:
Q = injection flow rate, h = preform thickness, ϕ = porosity

Rearranging eq. 1 provides the sensor time as a function of the fluid flow front shape and the experimental parameters:

$$t = \frac{d^2\left[1+(a/b)^2 \tan^2(\alpha-\theta)\right]}{m_1(a/b)\left[1+\tan^2(\alpha-\theta)\right]} - \frac{r_o^2+c}{m_1} \tag{3}$$

In eq. 3, parameters d and α are known for each sensor. Parameter m_1 is known once the injection flow is set, and the preform thickness and porosity are chosen. Each sensor trigger time t is measured and recorded by the data acquisition system. Thus eq. 3 can be written for each sensor, providing an over specified set of equations for the unknowns: a/b, θ, and c. The best fit values of (a/b), θ and c are found through iteration.

After the flow front shape is found, the inlet pressure information is used to find the principal components of the permeability tensor. For constant injection rate, the increase of the mold inlet pressure over time is closely approximated by [7]:

$$P_{in} = \frac{\mu Q}{4\pi h K_{rr}} \ln\left(1+\frac{Qt}{\phi \pi h r_0^2}+\frac{c}{r_0^2}\right) \tag{4}$$

Where:
P_{in} = inlet pressure , K_{rr}= geometric mean of K_{xx} and K_{yy}, $\sqrt{K_{xx}K_{yy}}$

Eq. 4 differs from previous derivations [7] because the parameter c is included to account for non-ideal entrance effects.

Plotting P_{in} vs. $\ln(1+\frac{Qt}{\phi \pi h r_0^2}+\frac{c}{r_0^2})$ results in a line of slope, $\frac{\mu Q}{4\pi h K_{rr}}$, from which K_{rr} is obtained. As K_{rr} is equal to the geometric mean of K_{xx} and K_{yy} and to (a/b), $(a/b) = \sqrt{K_{xx}/K_{yy}}$, the individual values of K_{xx} and K_{yy} are easily found.

RESULTS AND DISCUSSION

Basalt Permeability

The basalt in plane permeability data is shown in Table 2. The data in each cell is given as average ± standard deviation. The unit for permeability is length^2, and 1 m^2 = 1.01325 × 10^{12} Darcy [11]. The angle θ, between the warp direction of the fabric and the permeability principle axis (the one with larger permeability values), is defined as clockwise from the former to the latter, seen from above.

The results derived from the sensors in the bottom and top plates correspond well together corresponding to good fluid flow in all basalt layers uniformly. The square root of the permeability anisotropic ratio is just slightly larger than 1, which also corresponds well with visual observations of the anisotropic ratio of the elliptical flow front. At 35.8% fiber vol. %, the alignment of the principle axis for the basalt fabric, K_{xx}, is quite close to the warp direction, as indicated by the small angle θ in Table 2.

Table 2. In-plane permeability results for basalt fabric

	Anisotropic ratio of permeability (l^2)	Angle θ, Deg	K_{xx}, Darcy	K_{yy}, Darcy
Bottom Plate Data	1.374 ± 0.097	-3.47 ± 5.60	857.85 ± 218.88	625.71 ± 174.19
Top Plate Data	1.389 ± 0.091	-6.34 ± 6.35	858.43 ± 227.46	617.98 ± 166.71

The statistical distribution of the basalt permeability data is shown in Figure 3.The anisotropic ratio ('a' in Figure 3c) of the basalt fabric has a much smaller standard deviation than observed in previous measurements where sufficient data was collected to generate reliable statistics. This smaller standard deviation may be related to a high correlation between K_{xx} and K_{yy}. To determine the correlation between K_{xx} and K_{yy}, plots as shown in Figure 5 were constructed. Because the permeability principal axis is very close to the warp direction, we use K_{warp} to represent K_{xx} and K_{weft} to represent K_{yy}.
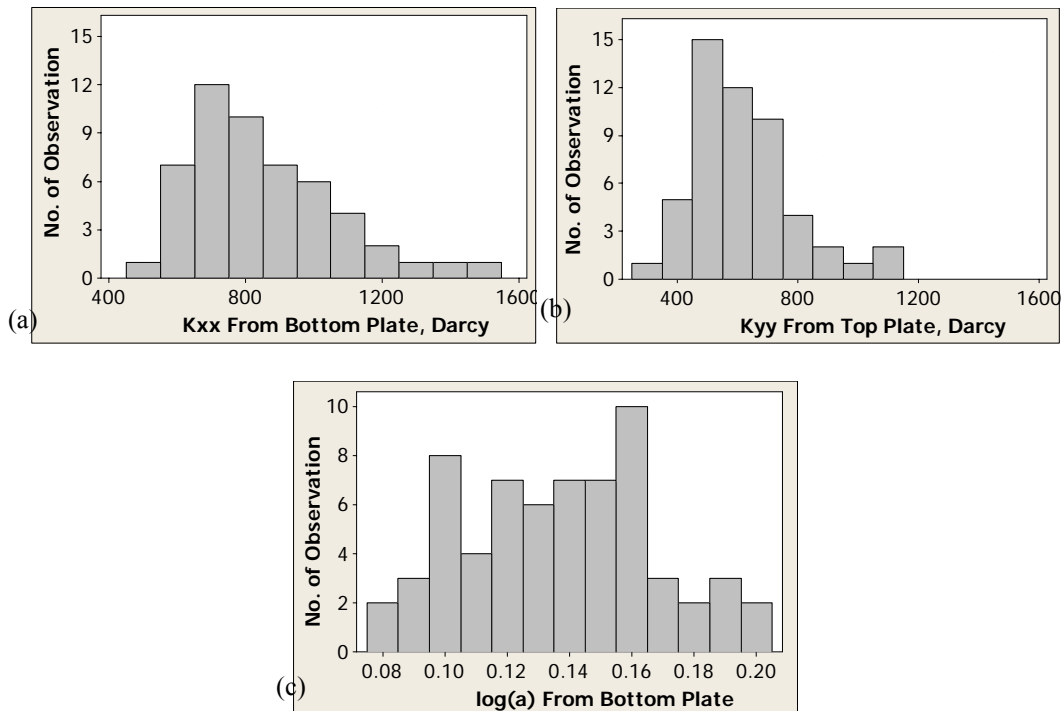
Figure 3. Permeability Distribution

For basalt, a large correlation coefficient, R^2, between K_{xx} and K_{yy} is shown in Figure 4a and compared to Figures 4b and 4c of R420 and RE 144/255 glass fabrics [1]. Glass fabric, RE 144/255 (Figure 4c), has a much smaller correlation between K_{warp} and K_{weft}, compared to the

basalt fabric where as R420 glass fabric (Figure 4b) has negligible correlation. The t-test is used for all three fabrics to determine if the correlation between K_{warp} and K_{weft} is significant. After the t statistic was calculated, the P-value associated with that t statistic was found from the t probability distribution. The P-value provides the confidence level in the (significance) correlation coefficient. For example, the P-value of the correlation coefficient of basalt fabric is less than 0.001, which means that this correlation coefficient is significant at a greater than 99.9% confidence level. (More precisely, there is less than 0.1% chance of being wrong by rejecting the hypothesis that the correlation coefficient is insignificant). With similar reasoning, we find that the correlation coefficient for RE144/255, a 2/2 twill glass fabric, is also significant with a greater than 99.9% confidence level. However, the P value for the R420 plain weave glass fabric is 0.327. This means that the correlation coefficient between K_{warp} and K_{weft} is not significant for the R420 fabric.
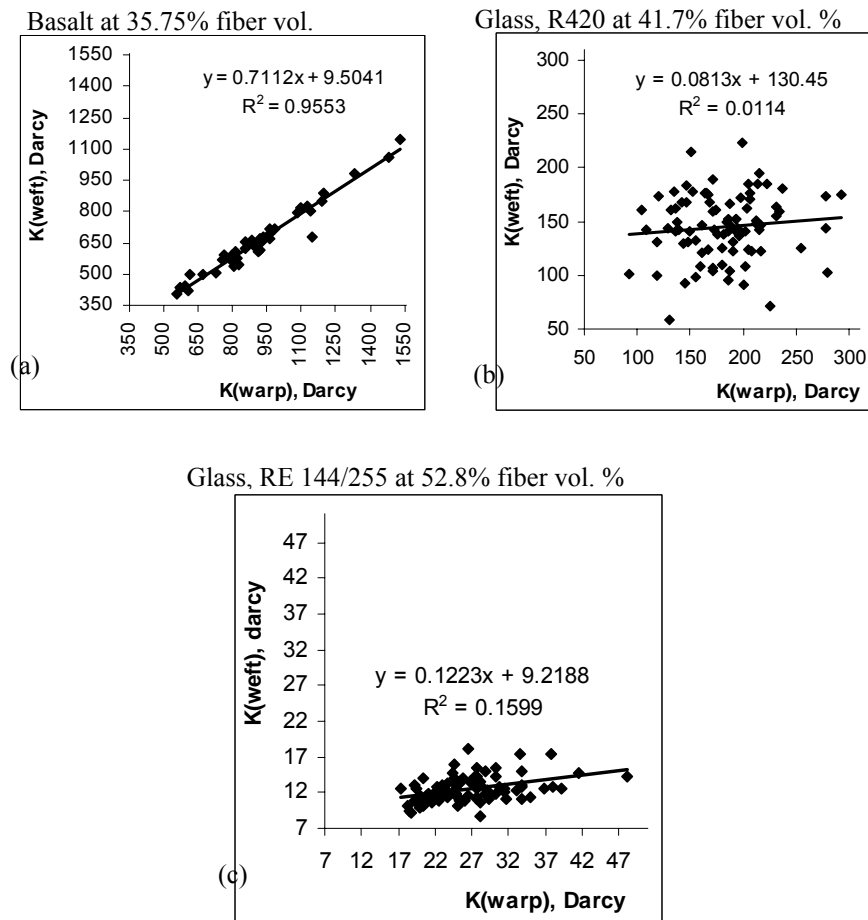

Figure 4. Permeability correlations in warp and weft directions for different fabrics.

Such large differences in the correlation coefficients between these fabrics may be caused by the difference in the fabric structures. It is known [1] that broad permeability distributions can result from the nesting of yarns in the neighboring layers (or the relative shifts between neighboring layers). For the fabrics discussed above, nesting probably causes the broad distribution of the components of the permeability tensor. However, nesting appears to have different effects on the distribution of the permeability anisotropy, depending upon the fabric structure. Plain weave R420 has the broadest distribution of anisotropy and basalt twill fabric the narrowest.

The high correlation between K_{warp} and K_{weft} for basalt fabric is desirable for RTM processing because a consistent flow pattern will be obtained. In the cases where a broad distribution of anisotropy is obtained and there is little correlation between K_{warp} and K_{weft}, variable flow patterns may occur for different injections, rendering control and part-to-part consistency difficult to achieve.

CONCLUSIONS

A new sensor system and data analysis procedure to derive flow pattern was developed for the in-plane permeability measurement with expected use for electrically conductive reinforcement. This apparatus can be used to calculate the flow front orientation angle in addition to the anisotropy and principal components of the permeability tensor. Measurements of the permeability of basalt woven twill showed that our experiments are reproducible and consistent with previous work. These measurements reveal that different fabric structures may have very different anisotropy distributions even when the distributions of the components of the permeability tensor are similar. Fabrics with a high degree of correlation between permeability components and a small variability in anisotropy are expected to be easier to process.

ACKNOWLEDGEMENTS

REFERENCES

1. Kris Hoes, PhD Thesis, Vrije Universiteit Brussel, Brussels, (2003).
2. (a) K. L. Adams, W. B. Russel and L. Rebenfeld, International Journal of Multiphase Flow, 14 (2), 203-215 (1988). (b) Jingyi Xu and Yulu Ma, China Plastics, 6 (1), 9-16 (1992).
3. L. Baichen, S. Bickerton and S. G. Advani, Composites, 27A (2), 135-141 (1996).
4. R. S. Parnas, Liquid Composite Molding, Carl Hanser Verlag, Munchen, 2000, 5
5. F. A. L. Dullien, Porous Media: Fluid Transport and Pore Structure, 2nd Ed., Academic Press, Inc. San Diego, California, 1992, pp. 6
6. T. A. K. Sadio, S. G. Advani, R. S. Parnas, International Journal of Multiphase Flow, 21 (5), 755-774, (1995).
7. T. Kruckenberg and R. Paton, Resin Transfer Molding for Aerospace Structures, Kluwer Academic Publishers, Dordrecht, The Netherlands, 1998, pp. 196
8. J.-F. Delerue, S. V. Lomov, R. S. Parnas, I. Verpoest, M. Wevers Polymer Composites, 24 (3), 344-357, (2003).
9. (a) R. S. Parnas and A. J. Salem, Polymer Composites, 14 (5), 383-394 (1993). (b) P. Ferland, D. Guittard and F. Trochu, Polymer Composites, 17 (1), 149-158, (1996). (c) R. Gauvin, et. al., Polymer Composites, 17 (1), 34-42, (1996). (d) R. B. Gebart and P. Linström, Polymer Composites, 17 (1), 43-51, (1996). (e) T. S. Lundström, et. al., Composites, 31A (1), 29-43, (2000).
10. Kris Hoes, et. al., Composites, 33A, 959-969, (2002).
11. R. Pan et al., Polymer Composites, 21 (6), 996-1006, (2000).